Shuangxinfang prevents S100A9-induced macrophage/microglial inflammation to improve cardiac function and depression-like behaviour in rats after acute myocardial infarction

Yize Sun (18765800272@163.com)
BUCM
Zheyi Wang
Shandong University
Jiqiu Hou
Dongfang Hospital
Jinyu Shi
Beijing University of Chinese Medicine
Zhuoran Tang
Beijing University of Chinese Medicine
Chao Wang
Dongfang Hospital
Haibin Zhao
Dongfang Hospital

Research

Keywords: Shuangxinfang, traditional Chinese medicine, acute myocardial infarction, depressive disorder, S100A9, inflammation, microglia, macrophages

Posted Date: November 2nd, 2021

DOI: https://doi.org/10.21203/rs.3.rs-958964/v1

Abstract

Background

Depression is a common complication of cardiovascular disease, which deteriorated the cardiac function. Shuangxinfang (Psycho-cardiology Formula, PCF) was reported to alleviate myocardial ischemia injury and improve depression-like behavior. Interestingly, our previous proteomics study predicted that the protein S100A9 appeared as an important target, and macrophage/microglial inflammation might be involved in the process of PCF treating depressive disorder induced by acute myocardial infarction (AMI). The aim of this study is to validate the proteomics results.

Methods

AMI rat models were established *in vivo*, followed by the administration of PCF or ABR-215757 (also named paquinimod, inhibiting S100A9 binding to TLR4) for 5 days. Forced swimming test (FST) and open field test (OFT) were applied to record depression-like behavior, and echocardiography was employed to evaluate cardiac function. Morphological changes of cardiomyocytes were assessed by HE staining and TUNEL staining on day 7 after cardiac surgery, as well as masson trichrome staining on day 21. Hippocampal neurogenesis was determined by Nissl staining, while 5-hydroxytryptamine (5-HT) and brain-derived neurotrophic factor (BDNF) in the hippocampus were detected as biochemical indicators of depression. Myocardial and hippocampal expression of inflammatory factors were analyzed by western blotting, immunofluorescence, and ELISA. The activation state of macrophage and microglia was assessed via immunoreaction respectively using CD68 and Iba1. For *in vitro* confirmation, BV2 cells were primed with recombinant protein S100A9, and then pretreated with PCF serum, to determine alterations in microglial activation and inflammation.

Results

Rats in the AMI group showed heart function deterioration, as well as depression-like behavior. Coronary ligation not only brought about myocardial inflammation, cell apoptosis and fibrosis, but also reduced the neurogenesis and decreased the content of 5-HT. PCF could ameliorate the pathological and phenotypic changes of the heart and brain, and inhibited the expression of S100A9/TLR4/NF-κB pathway, the activation of microglial cell and the secretion of IL-1β and TNF-α raised by AMI. ABR-215757 showed therapeutic effect and molecular biological mechanisms similar to PCF. Pretreatment with PCF serum *in vitro* was proved to efficiently block the hyperactivation of BV2 cells and increasement of cytokine contents induced by recombinant protein S100A9.

Conclusion

We identify S100A9 as a novel and potent regulator of inflammation in both heart and brain. Macrophage/microglia inflammation mediated by S100A9 is considered as a pivotal pathogenic in depression post-AMI, as well as a major pathway for the treatment of PCF, suggesting that PCF is a promising therapeutic candidate for psycho-cardiology disease.

Background

The reported prevalence of depression after acute myocardial infarction (AMI) for the last few years varied across studies and generally ranged from 18–40%[1–4]. The TRIUMPH study, an observational multicenter cohort study published in *Circulation*, which enrolled 4062 patients with AMI and recognized depression between 24-72 hours of admission, declared that one-fifth of patients with AMI had significant depressive symptoms[2]. A research assessed depression in patient survivors during hospitalization, at 3 months and 12 months after AMI, and the three groups presented almost equal representation of depression according beck depression inventory (BDI) with 34.1%, 30.8% and 30% respectively [3]. These results implied that acute coronary event might directly induce depression, regardless of other socioeconomic factors. It's reported that only patients with incident post-AMI depression, rather than ongoing or recurrent depressions, have an impaired cardiovascular prognosis[5], suggesting that the pathological mechanism of AMI- induced depression may be different from other types and worthy of further exploration.

Depression has been classified as a risk factor for poor prognosis among patients with cardiovascular diseases, which is closely related to decreased heart rate variability, sympathetic nervous excitement and ventricular arrhythmias, ulteriorly leading to fatal and non-fatal cardiovascular events, loss of life quality, as well as an increase in healthcare expenditure and suicide risk[6–11]. Selective serotonin reuptake inhibitors (SSRI) are currently a preferred choice for depressed patients with cardiovascular disease. However, associations of antidepressant treatment with long-term cardiac outcomes in depression following AMI have therefore been inconclusive[12–15]. It means that new therapeutic strategies still need to be developed to make up for the deficiency of current antidepressants.

Shuangxinfang (Psycho-cardiology Formula, PCF) consists of four kinds of herbs, including Salvia miltiorrhiza, Rhizoma chuanxiong, Semen ziziphi spinosae and Lily bulbs, which is beneficial to promote blood circulation and remove stasis, as well as lift the spirit and gain the vitality to be away from gloomy mood and somatic distress. Our previous clinical trials have already confirmed that PCF could relieve angina pectoris and improve depressive symptoms[16]. Furthermore, the pharmacological mechanism of PCF is concentrated on regulation of inflammatory response and neuroendocrinology system. PCF could inhibit the expression of inflammatory factors such as tumor necrosis factor-α (TNF-α) in AMI rats, and meanwhile appease the neural system by modulating the γ-aminobutyric acid (GABA) system[17]. The above data highlighted a critical role for the PCF in inhibiting inflammation caused by injured myocardium and alleviating depression following AMI.

To systematically explore the biological mechanism of PCF in the treatment of depression after AMI and identify possible targets, we have performed pharmacoproteomic profiling of myocardium and hippocampus in rats from the sham, the AMI, and the PCF group using Label-free liquid chromatography-mass spectrometry (LC-MS/MS). The mass spectrometry proteomics data have been deposited to the ProteomeXchange Consortium. The intersection of differentially expressed proteins (DEPs) in peri-infarct border zone and hippocampus produces a unique protein, that is S100A9, which has become a topic molecule in the cardiovascular field during these years [18–20]. According to alteration of the proteomics profile in biological fraction and pertinent pathways, macrophage/microglia inflammation might be biological mechanisms for PCF to protect against the pathological progress of depression post-AMI. As reported, S100A9 modulates macrophage inflammation in AMI, as well as regulates microglial inflammation in depression[21, 22], yet the evidence of it is not quite adequate in depression post-AMI. Indeed, it guides a direction for molecular mechanisms in the psycho-cardiology diseases. In this study, systematic experiments were performed in AMI rats with depression-like behavior to verify the hypothesis derived from proteomics.

Materials And Methods

Drugs and reagents

PCF was purchased from Beijing Pharmaceutical Co. Ltd. One dosage of PCF composed of: Salvia miltiorrhiza 20 g, Rhizoma chuanxiong 12 g, Semen ziziphi spinosae 30 g and lily bulb 30 g. One dosage of PCF was dissolved in 100 ml distilled water. The optimal lavage dose was 1ml/100g/d according to preliminary tests[17]. Paquinimod (Apexbio, Houston, USA), also called ABR-215757 (a specific inhibitor of S100A9), binds to S100A9 in a Ca^{2+}/Zn^{2+} dependent way and blocks interaction with TLR4[23, 24]. It has been applied to the experimental research of depression, atherosclerosis and other diseases[25, 26]. According to the literature and the results of previous studies, ABR-215757 was successively dissolved in 10% DMSO, 40% polyethylene glycol 400 (PEG400), 5% Tween 80 and 45% normal saline, and injected intraperitoneally at a dose of 5mg/kg/d, once a day for 5 consecutive days[27, 28]. Recombinant protein S100A9 (Bio-Techne, Minnesota, USA) was prepared into 300μg/ml mother solution with sterile water, and then diluted to 0.01μM, 0.02μM, 0.05μM and 0.1μM with complete medium in the initial experiments. A concentration of 0.1μM was adopted in the subsequent experiments. C34 (Apexbio, Houston, USA) inhibited toll-like receptor 4 *in vitro*, which was dissolved in DMSO to prepare mother liquor with a concentration of 10mM and diluted to the final concentration of 10μM when used[29]. Ferulic acid (yuanye Bio-Technology, Shanghai, China) was dissolved in DMSO and configured to a concentration of 80μM.

In vitro **study**

Preparation of medicated sera

The rats were given PCF or distilled water as above, and anesthetized by intraperitoneal injection of pentobarbital one hour after administration. Blood was collected from the abdominal aorta and

centrifuged, then heat-inactivated at 56℃ for 30min and filtered by a 0.22 μm filter membrane. The serum was packed separately and frozen at -80℃ until use.

Cell culture

The microglial cell line BV-2 was received from Scientific Research Center of Shanghai Tenth People's Hospital and cultured in high-glucose Dulbecco's-modified eagle's medium (H-DMEM, Invitrogen, USA) with 10% fetal bovine serum (FBS Gibco, USA) and 1% penicillin/streptomycin (Gibco, USA) at 37˚C in a humidified atmosphere with 5% CO2. Cells at 80% confluency were supplied for experimental treatments or trypsinized for passage.

Group design

BV2 microglia cells were divided into 6 groups: control group, recombinant protein S100A9 group, C34 group, PCF serum (PCF) group, ferulic acid (FA) group and control serum (CS) group. Except for the control group treated with complete medium, cells in C34 group, FA group, PCF group and CS group were cultured in 0.1μM of recombinant S100A9 protein for 6h, followed by complete medium respectively supplemented with 10μM C34, 80μM FA, 5% PCF serum and 5% control serum for 6 h.

CCK-8 assay

Cells were cultured in 96-well plates (2 ×10^4 cells per well) with 100 μl complete medium containing various doses of recombinant S100A9 protein (0.01/0.02/0.05/0.1μM), control serum (5%, 10%, 20%) or PCF serum (5%, 10%, 20%), to determine the dose-dependent effects of reagents. Cell viability was measured via the CCK-8 assay kits. The absorbance at 450 nm was measured with a microplate reader.

Enzyme linked immunosorbent assay (ELISA)

The cell supernatants from each sample were collected for ELISA assays, as well as myocardium and hippocampus. Concentrations of inflammation marker including S100A9, TNF-α and IL-1β were determined by pre-coated ELISA kits (Mlbio, Shanghai, China) according to the manufacturer's instructions.

In vivo **experiment**

Animals

Male Sprague-Dawley (SD) rats were purchased from Beijing Vital River Laboratory Animal Technology Co. Ltd. (License No. SCXK (Beijing) 2016–0006). All rats were fed in a specific pathogen–free facility with controlled temperature (22 ± 1°C), relative humidity (65–70%), and a 12:12 light/dark cycle.

Establishment of AMI rat model

As described previously, ligation of the left anterior descending (LAD) coronary artery was used to construct AMI rat model, while only threading was operated without knotting in the sham group[17, 30]. Penicillin was injected intraperitoneally to prevent from infection. The success of AMI model was marked

of pathological Q wave by more than 6 leads of ECG I, AVL and V1~V6 in electrocardiograph on the second day after surgery.

Design and allocation

The rats were randomly divided into the sham group, AMI group, PCF group and ABR-215757 group. Rats in PCF group were administered intragastrically PCF solution once a day for 5 days, while the rats in the sham and AMI group received the same volume of distilled water on the same schedule. Paquinimod was injected into the rats of ABR-215757 group intraperitoneally. After the last treatment administration, the rats underwent behavioral tests and echocardiography. Then a half of the rats randomly selected were sacrificed to remove heart and brain tissues. On the 21th day post-surgery, the remaining rats were sacrificed for detecting neurogenesis in the hippocampus, as well as cardiac fibrosis in the myocardium.

Behavioral tests

Behavioral tests were performed in a double-blinded manner and operated in a dark and quiet room, and all rats were transported to which one hour earlier to acclimatize. The behavior in OFT (open-field test) and FST (forced swimming test) was videotaped and further analyzed by Supermaze (Softmaze, Shanghai, China), a specialized animal behavior video analysis software.

Open-field test (OFT)

The first step was to set up the software program. In Supermaze, grayscale was set as the recognition algorithms and three points were determined to track the position of the rats. The open field is a square wooden chest (100 cm*100 cm*60 cm) with a black floor and divided into 25 identical areas with white lines. A single rat was placed in the central square and allowed to move freely for 5min. The number of verticality (times of rat stood on its hind limbs) was recorded by an observer blind to the group, while the total distance and distance in central region were recorded in the software. The field was wiped clean with 75% alcohol before each test.

Forced swimming test (FST)

Dynamic background method was selected and the rats were located by the center of gravity in Supermaze. The FST was operated in a transparent glass cylindrical tank with 60cm in height, 38cm in width and 40cm in depth. Rats were put into the glass tank filled with 22~24°C fresh water, and allowed to swim freely for 5min. The immobility time was recorded by the video camera and analysed by Supermaze software.

Echocardiography

The rats were anesthetized and fixed on a board with fur shaved. Three continuous cardiac cycles were captured from the left ventricular short axial section to detect the M-shaped curve. Left ventricular ejection fraction (LVEF) and left ventricular fractional shortening (LVFS) were measured to assess cardiac function. The left ventricular end-diastolic inner diameter (LViDd), left ventricular end-systolic inner

diameter (LViDs), left ventricular end-diastolic volume (LVEDV) and left ventricular end-systolic volume (LVESV), were measured to evaluate the ventricular structure.

H&E and Masson staining

The tissues extracted were embedded in paraffin and cut at a 4 μm thickness after fixation in 10% neutral formalin for 72h. These slices were stained with Hematoxylin/Eosin (H&E) or Masson trichrome and observed under an optical microscope (Carl Zeiss Microscopy, Germany), to evaluate histopathological changes and collagen deposition. The area percentage of collagen deposition were analyzed by the ratio of fibrosis area to the total myocardial area.

Nissl Staining

The brain was dyed with toluidine blue o to assess neurogenesis. Brain sections were immersed in xylene, and then rehydrated in graded alcohol solutions and distilled water. Subsequently, tissue slices were stained by toluidine blue (Servicebio, Wuhan, China) for 10 min, quickly rinsed in distilled water, dried at a 60°C environment, made transparent by xylene, and sealed with neutral gum. Three sample sections were selected from each group, and observed using an optical microscope. The mean integrated optical density (IOD) of dentate gyrus (DG) region in hippocampus was measured by Image-Pro Plus 6.0 software (Media Cybernetics Inc., Rockville, MD, USA).

TUNEL assay

Cardiac cell death was evaluated utilizing a TdT-mediated dUTP nick end labeling (TUNEL) assay kit (Roche, USA) in accordance with the manufacturer's protocol. The kit was labeled with FITC fluorescein, and the positive apoptotic nucleus was dyed green. The cells were stained with DAPI (1:30, Beyotime Biotechnology, China) for nuclear counterstaining and observed under fluorescence microscope (Zeiss Axio Scope A1). Three fields of each slice were selected for quantification. Image J software (NIH, MD, USA) was applied to calculate the number of tunel positive cells. Apoptosis index (AI) = (number of apoptotic nucleus/number of total nucleus) × 100%.

Immunofluorescence staining

Paraffin sections of heart and brain tissue were processed as previously described. After routine dewaxing, hydration and antigen retrieval, the tissues were incubated in bovine serum albumin (BSA) for 30min. After blocking, the slices were incubated with an anti-Iba1 (1:500, Abcam, UK), anti-CD68 (1:200, Abcam, UK), or anti-S100A9 (1:500, Proteintech, USA) primary antibody overnight at 4°C, followed by secondary antibodies conjugated to CY3 (1:300, Servicebio, China) or HRP (1:500, Servicebio, China). As for anti-S100A9, the slices were incubated with FITC at room temperature in dark for 10 minutes. Subsequently, the tissues were stained with DAPI for nuclear counterstaining. The stained slides were photographed under fluorescence microscope. The number of $CD68^+$ cells in the myocardium or $Iba1^+$ cells hippocampus was counted by ImageJ software (NIH, MD, USA) in a blinded manner. The data were expressed as the mean number of cells per square millimeter. For intensity measurements, three sections from each sample at the same level were used to determine the mean optical density (mean optical

density = IOD/area). The mean values were calculated from 3 randomly selected microscopic fields from each section.

Western blotting

The hippocampal and myocardial samples were lysed, then proteins were extracted with RIPA buffer (Thermo Fisher Scientific, USA) and measured by the BCA protein concentration Determination kit (Glpbio, USA). Protein mixtures were separated via 10% SDS-PAGE and transferred to polyvinylidene difluoride (PVDF) membranes (Millipore, USA). TBST containing non-fat dried milk was used to block non-specific binding to the membranes, and the membranes were incubated with primary antibodies at 4°C overnight, followed by incubation with the secondary antibodies (1:3000, Thermo Fisher Scientific) at room temperature for 30 min and reaction with enhanced chemiluminescence (ECL). The primary antibodies for immunoblotting were as follows: anti-S100A9 (1:1000, Proteintech), anti-TLR4 (1:1000, Abcam), anti-NF-κB (1:1000, Abcam), anti-BDNF (1:1000, Abcam), anti-GAPDH (1:1000, Servicebio), and anti-ACTIN (1:1000, Servicebio). The exposure condition was adjusted on the basis of luminescence intensity. The results were scanned and colour-modulated, and the target band intensities were analyzed by the BandScan software (Glyko, USA).

LC–MS/MS method

The hippocampus tissue samples were weighed and ground in the frozen grinding machine. 80% methanol was added at a ratio of 1:10, followed by vortex, low-temperature ultrasound for 10min, and centrifugation at 13000rpm for 10min. Then supernatant was removed to frozen centrifugation and concentrated to dry, and 100ul of solvent was added for redissolution. The analysis was performed on the AB SCIEX QTRAP 4500 (USA) triple quadrupole mass spectrometer in SRM and positive ionization mode. The LC separation was run on an ACQUITY HSS PFP column (2.1×100mm, 1.7μm, USA) equipped with a Waters ACQUITY UPLC I-Class infinite binary pump. Acetonitrile containing 10mM amine acetate and 0.1% formic acid was used as solvent A, and water containing 10mM amine acetate and 0.1% formic acid was used as solvent B. The flow rate was 0.2 ml/min. The steps of gradient elution were as follows. The initial conditions were 98% solvent B starting from 0 minutes, 8 minutes to 0% solvent B, returning to the initial state of 98% solvent B after 2 minutes, 12 minutes to end a collection. The column temperature was 35°C, while the sample was kept at 10°C and the injection volume was 10μl. The MS parameters were as follows. ESI ion source temperature 500℃; Air curtain 30 psi; Collision activated dissociation gas settings: Medium; ion spray voltage: 5500V. All data was processed by Analyst 1.6.3 Software.

Statistical analysis

The data was presented as mean ± SEM. Statistical graphing was performed using GraphPad Prism software (version 8.0; Inc., San Diego, CA, USA). For multiple comparison tests, one-way analysis of variance (ANOVA) was performed followed by a Tukey *post hoc* test. For all analyses, an average value of $P < 0.05$ was considered statistically significant.

Results

PCF improved cardiac function and ventricular remodeling in AMI rats

As shown in Fig. 1, myocardial infarction led to wall thinning, dilated left ventricular chambers and an obvious decrease in cardiac function. The LVEF and LVFS were decreased in the AMI groups compared with the sham group ($P < 0.05$). In contrast, the LVEF and LVFS in the PCF group and ABR-215757 group were significantly elevated compared to the AMI group ($P < 0.05$). Thus, PCF overcame the inhibitory effects of AMI on the LVEF and LVFS. The LVIDd and LVIDs respectively indicated end-diastolic and end-systolic left ventricle (LV) internal dimension, while LVESV and LVEDV respectively showed the maximum volume of the ventricle in systole and diastole. The four indicators in the PCF group and ABR-215757 group were declined compared to the AMI group ($P < 0.05$).

PCF alleviated histological injury in myocardial tissue of AMI rats

The severity of cardiac damage was evaluated by morphological observations (Figure 2). Hematoxylin–eosin staining showed orderly arrangement of myocardial fibers in the sham group. Conversely, the myocardial fibers became loosely and irregularly arranged in the AMI group. Instead, PCF and ABR-215757 alleviated the morphological injuries after AMI. Compared with the sham group, apoptosis index was significantly increased in the AMI group on day 7 after coronary ligation, then a large number of fibrotic scar was observed on day 21. TUNEL assay revealed that PCF and ABR-215757 significantly ameliorated AMI-induced cell apoptosis ($P<0.01$, Figure 2B and 2D), and masson staining showed that both of them significantly decreased the fibrosis area in peri-infarct border zone, indicating their beneficial effects to reduce impairment of cardiac function.

PCF improved depression in rats after AMI

Compared to the sham group, rats in the AMI groups showed depression-like behaviors, such as reduction of crossing zones and rearing times in OFT, as well as longer immobility time in FST ($P < 0.05$, Fig. 3). However, rats in the PCF group were much more active in OFT, and rats after intraperitoneal injection of Paquinimod had a much shorter immobility time in FST.

The mainstay of antidepressant therapy still directs at serotonin (5-hydroxytryptamine, 5-HT) metabolism, in detail, blocking reuptake of 5-HT from the extracellular space. Tryptophan, as a precursor for serotonin, 95% of it is degraded in the liver through the kynurenine pathway, and the remaining is used for the synthesis of 5-HT[31]. Abnormalities in the tryptophan-kynurenine pathway are implicated in the pathophysiology of depressive disorder[32]. To examine the effects of AMI on neurotransmitters in the brain, we analyzed the hippocampus tissues by liquid chromatography-mass spectrometry (LC-MS). As shown in Fig. 4A, a significant decrease in 5-HT level was observed in AMI rats, while PCF and ABR-215757 treatment led to a degree of recovery. The level of tryptophan (Try) was altered in a manner

similar to that of 5-HT. Proinflammatory cytokines catalyzes the conversion of Try to kynurenine (Kyn), and the kynurenine pathway may elucidate the phenomenon of inflammation in depression[33]. It has evoked widespread concern that the ratio of kynurenine to tryptophan is significantly enhanced in patients with depression[34, 35]. Our results showed an increased hippocampal Kyn/Try ratio in AMI group and the ratio declined with the administration of PCF or S100A9 inhibitors (Fig. 4B).

Depression is associated with neuroplasticity in the brain regions, particularly the hippocampus. Nitensite, easily stained by toluidine blue, reflect the synthesis of Nissl bodies and the survival of nerve cells. Nissl staining revealed that, the rats had fewer neurons with loose arrangement in the hippocampal DG regions (Fig. 4C), whereas no obvious hippocampal neuron loss was observed in the PCF group and ABR-215757 group on day 21 after coronary artery ligation. Brain-derived neurotrophic factor (BDNF), a topic neurotrophic factor of intensive research in the mammalian brain, contributing to the maintenance and survival of neurons, as well as activity dependent regulation of synapse number and function, is integral to the pathophysiology of depression[35]. Multiple lines of evidence implied that administration of BDNF into either hippocampus or midbrain in rodent models produces an antidepressant-like effect[36]. In this study, the expression level of BDNF was downregulated in AMI group compared to the sham group, and showed an upward trend after administration of PCF and ABR-215757, but there was no statistical significance between groups (Fig. 4D).

PCF inhibited the expression of S100A9/TLR4/NF-κB signaling pathway

Our present proteomic study revealed that S100A9 was the only molecule intersected from numerous proteins in the myocardium and hippocampus, as well as one of the differentially expressed proteins among the sham, AMI and PCF treatment groups. We first verified the *in vivo* effect of coronary ligation on the S100A9 expression by immunoblotting analysis. Consistent with proteomic data, the expression level of S100A9 protein was elevated in AMI group compared to the sham group and was returned to the basal level by PCF treatment (n = 3 per group, Fig. 5A-5B). In addition, the expression level of TLR4 and NF-κB proteins were changed in a manner similar to that of S100A9. Interestingly, the protein expression trend was observed not only in myocardium but also in hippocampus. To explore the effect of S100A9 on inflammatory factors, ABR-215757 group was set and the expression pattern was found to be parallel to that in PCF group. But it's regrettable that there was no statistically significant difference in protein expression between groups. Expression of S100A9 protein the hippocampus was also visualized by immunofluorescence. Expression analysis showed increased expression of S100A9 in AMI group, and S100A9-positive fluorescence intensity were markedly decreased in PCF and ABR-215757 group (Fig. 5C-5D).

PCF reduces the contents of proinflammatory factor

Furthermore, we detected S100A9 expression in the hippocampus and myocardium by means of ELISA. As shown in Fig. 6, S100A9 levels in the myocardium were significantly increased in the AMI group ($P <$

0.01), while those in the sham group remained low. PCF administration reduced myocardial S100A9 level compared with the AMI group ($P < 0.05$). Compared with the sham group, coronary ligation not only significantly increased the IL-1β and TNF-α levels in myocardium, but also elevated the levels of inflammatory factors in hippocampus to promote neuroinflammation.

PCF inhibits the activation of macrophages/microglia

CD68 and Iba1 is recognized as a specific marker respectively for macrophage and microglia. To investigate the effect of AMI on the activation of macrophage in the heart, immunofluorescence staining for myocardial sections was performed. Results indicated that acute myocardial ischemia significantly increased the activation of macrophage and accordingly the number of CD68 positive cells was increased (Fig. 7A-B). However, PCF and ABR-215757 treatment inhibited macrophage activation and decreased the number of $CD68^+$ cells. We further interrogated the effect of cardio-surgery on hippocampal microglia. As results indicated, hippocampal microglia were activated by coronary ligation, while PCF and ABR-215757 treatment decreased the number of $Iba1^+$ cells in the hippocampal region (Fig. 7C-D).

The effect of recombinant protein S100A9 on the viability of BV2 cells

CCK-8 assay was applied to determine the effect of recombinant protein S100A9 on the viability of BV2 cells. As shown in Fig. 8A, the administration of protein S100A9 with 0.01μmol~0.05μmol for 6 hours had no significant effect on the viability of microglia cell, while 0.1μmol of S100A9 could observably promote microglial cell proliferation ($P < 0.05$). Therefore, 0.1μmol of S100A9 was utilized in the following experiments.

S100A9 induced morphological changes of microglia cells

As “sentinels” of the nervous system, it is fitting that microglia respond to changes of biological signaling. Further investigation in BV2 cells observed two major morphological phenotypes, amoeboid versus ramified (Fig. 8C). Resting microglia cells existed mostly with oblate bodies, as well as stretched and elongated synapses. Under the activation of recombinant S100A9 protein, microglia cells become enlarged, retract their processes, form new motile protrusions, and transform into spherical or ameboid form. Parameters such as cell area and radius can be used to describe microglia activation state. Then more detailed morphological characterization was carried out. The results revealed that compared with the control group, S100A9 induced decreases in radius ratio (Fig. 8D). These morphological modulations indicated the activation of microglia associated with the S100A9 stimulation.

Effect of PCF serum on S100A9-induced activation of inflammatory factors

This study investigates whether PCF serum is involved in suppression of the inflammatory response induced by S100A9. As shown in Fig. 8E, inflammatory factors including S100A9, TNF-α and IL-1β were markedly increased following treatment with recombinant S100A9 protein, compared with that in the control group (P<0.05). No marked reduction in inflammatory factors was observed in the control serum group, however, treatment with PCF serum resulted in a significant reduction in protein S100A9 (P<0.05). We have previously detected pharmaceutical ingredients in serum from rats intragastric by PCF utilizing LC-MS, and found that ferulic acid might be a major molecule component of PCF. Therefore, the inhibitory effect of ferulic acid on S100A9-induced inflammatory factors was also examined. The result turns out that ferulic acid can not only reduce S100A9 content, but also inhibit the expression of TNF-α and IL-1β (P<0.05). In addition, C34 (TLR4 inhibitor) was proved to reverse the proinflammatory effects of S100A9 (P<0.05).

Effect of PCF serum on the viability of BV-2 cells.

To confirm that the anti-inflammatory property of PCF serum was not due to cytotoxic effects on the BV-2 microglial cells, the drug serum group was further divided into three subgroups with concentration of 5%, 10% and 20% respectively. As can be seen from the Fig. 8B, the viability of the BV-2 cells was not reduced following treatment with low and medium concentrations of PCF. BV-2 cell viability was slightly decreased in high dose group, but there was no statistical significance compared with the control group. These results indicated that the inhibitory effects of drug serum to the S100A9-induced inflammatory response did not result from its cytotoxic action.

Discussion

Related proteins and immunoinflammatory phenotype predicted by previous proteomics were examined in this study. Our research highlighted that PCF inhibited macrophage/microglia inflammation by the suppression of S100A9/TLR4/NF-κB signaling after AMI, thus improving cardiac function and depression-like behavior. PCF serum, as well as ferulic acid, alleviated microglia inflammation *in vitro*.

According to proteomics results from our previous studies, we speculated that PCF may regulate S100A9 over-activation of macrophage/microglia inflammation, leading to a mitigation in subsequent inflammatory processes involved in AMI. The dramatic cardiomyocyte death initiates a cascade of inflammation in AMI, in the process of which, the role of alarmin S100A9 in deteriorating cardiac function has become a hot topic supported by several top journals of clinical and experimental evidence in these years[37–39]. S100A9, as a potent activator of the innate immune response, as well as the damage-associated molecular pattern (DAMP) protein, is abundantly expressed in neutrophils, and rapidly released from activated neutrophils, monocytes/macrophages and dying cardiomyocytes, into the coronary and systemic circulation after myocardial ischaemia[40]. S100A9 interacted locally with toll-like receptor 4 (TLR4) or receptor of advanced glycation endproducts (RAGE) to promote the expression of NF-κB and release IL-1β and TNF-α[41, 42]. The regulatory role of S100A9 in macrophage activation has been brought into focus. The continuous activation of macrophages might be actuated by S100A9

protein, which acts as a character at the center of the stage to orchestrate the functions of the individual players, in cooperation with other proinflammatory cytokines[39, 43]. Recently, Stankiewicz and colleagues analyzed the hippocampal transcriptome of mice subjected to acute and chronic social stress of different duration, and found that hippocampal S100A9 mRNA increased[44]. In addition, central injection of recombinant S100A9 proteins could evoke depressive-like behaviors, TLR4/NF-κB signaling activation as well as microglia activation, the effects of which were attenuated by TLR4 inhibitor TAK-242, indicating that the dysfunction of S100A9/TLR4 signaling in the hippocampus could generate neuroinflammation and depressive-like behaviors[45]. *In vitro* studies also showed that S100A9 observably increased the secretion of proinflammatory cytokines including TNF-α and IL-6 in cultured BV-2 microglial cells, the process of which was suppressed by TLR4 inhibitors[22]. Microglia activation is not only a hallmark of neuroinflammation, but also contributes to the development of depressive-like behaviors. Recent studies demonstrated that impairment of the normal structure and function of microglia, caused by either intense inflammatory activation can result in depression and associated impairments in neuroplasticity and neurogenesis. Accordingly, some forms of depression can be recognized as a microglial disease (microgliopathy)[46]. Similar to the above results, in AMI-induced depressive rats, the level of S100A9 showed an increasing trend in the myocardium and the hippocampus, accompanied by the activation of transcription factor NF-κB and the release of proinflammatory factors. Also, our research showed a higher content of S100A9 in the myocardium and the hippocampus by ELISA in the AMI group. Coronary ligation promoted the activation of macrophage/microglia, respectively evidenced by an increasement in the number of myocardial CD68 positive cells and hippocampal IBA1 positive cells. Intragastric administration of PCF down-regulated the expression of S100A9 and other inflammatory factors, as well as inhibited the activation of microglia. Our results revealed that PCF intervention inhibited inflammation, which might partly attribute to a reduction in the content of S100A9 and the inhibiting effect of macrophage/microglia activation.

For additional verification of the mechanism, ABR-215757 (paquinimod) was used for the inhibition of S100A9. Paquinimod exerted consistent and robust immunomodulatory effects on systemic lupus erythematosus, which has been positively evaluated in a phase 2 randomized controlled trial[47]. The application range of paquinimod has gradually expanded in preclinical studies, mainly lie in its inhibition of inflammatory reaction by blocking the interaction with TLR4 and RAGE[25, 48]. Paquinimod is second generation quinoline-3-carboxamides which show structural similarity to kynurenines, and might be a novel promising therapeutic way for depressive disorder[48]. At the moment, *in vivo* studies have demonstrated that ABR-215757 effectively ameliorates depressive symptoms[45]. In our research, after continuous administration of ABR-215757 in the whole acute phase, the expression level of S100A9 was significantly down-regulated, as well as NF-κB, IL-1β and TNF-α. Moreover, inhibition of macrophage/microglia activation by ABR-215757 was shown to alleviate inflammation and to modulate 5-HT metabolism. As a result of TLR4 signaling blocking, the depressive-like behaviors were successfully rescued and cardiac function was partially restored by ABR-215757 treatment.

However, it’s still not clearly identified that S100A9 induced an inflammatory response via the TLR4 receptor, nor that PCF inhibits microglial inflammation through this pathway. Therefore, we conducted cell

experiments, in which BV2 microglia was stimulated by recombinant S100A9 protein at a concentration of 0.1mmol to construct model groups. Our results showed that S100A9 could induce the release of IL-1β and TNF-α in microglial cells. Cellular morphology revealed the characters of recombinant S100A9 in the activation of microglia. An increase in IL-1β and TNF-α levels derived from activated microglia may promote the depressive symptoms. In addition, the C34 (TLR4 inhibitor) group and PCF (PCF serum) group were set up to elucidate the mechanisms that *in vivo* studies have failed to elucidate. The inhibition of TLR4 attenuated these effects of S100A9, indicating that S100A9-induced microglia activation depends on TLR4 signaling. We examined whether or not the expression of TNF-α and IL-1β induced by S100A9 was inhibited by the treatment with PCF serum using the BV2 microglia. The expression of inflammatory markers was significantly upregulated by S100A9, and showed a downward trend by the co-treatment with PCF serum.

In the infarcted myocardium caused by prolonged coronary occlusion, the damage-associated molecular pattern (DAMP) proteins released from necrotic cells trigger both myocardial and systemic inflammatory responses. Inflammatory cells clear the infarct of dead cells and matrix debris, as well as activate repair by myofibroblasts and vascular cells, but may also lead to adverse fibrotic remodelling of viable segments and accentuate cardiomyocyte apoptosis[49]. Induction of cytokines and up-regulation of endothelial adhesion molecules modulate leukocyte recruitment in the infarcted heart tissues. Apoptosis, a process of programmed cell death, has been proposed to occur in response to proinflammatory cytokines post myocardial ischemia[50]. In the present study, we measured the inflammation level and occurrence of apoptosis severally by HE staining and TUNEL staining in the heart tissues on day 7 after coronary ligation. Also, Masson staining was applied to assess myocardial fibrosis at 21 days post-AMI. In the AMI group, a severe inflammatory infiltrates and myocardial fibre rupture were shown, as well as increased apoptosis index and fibrotic region. Conversely, these pathological phenomenons were alleviated by the administration of PCF.

There is considerable evidence that behavioural impairment observed after AMI are consistent with a model of human post-MI depression[51–53]. A majority of studies accorded closely with the conclusion, and the team of Wann put a lot of efforts to make it convinced[52, 53]. As reported by Wann, MI rats display behavioural signs compatible with depression 2 weeks after the cardiovascular event, including anhedonia (i.e., less sucrose intake) and behavioural despair (i.e., decreased forced swimming)[52]. Our study declared that rats in AMI group showed depression-like behavior, as performed by reduced ability of movement in OFT and longer immobility time in FST. These findings implied that depression-like performance in rodents with MI was demonstrated by diverse behavioral tests.

Depression is recognized as a circuit disease influencing multiple encephalic regions that are connected in functional networks. The hippocampus, as a primary zone in cerebral limbic system, has been identified as a major role in the pathological progress of depression. Many factors that may interact with hippocampal damage to trigger depressive episodes, and neurotransmitter disturbance and altered neurotrophic signaling are included[54]. The 5-HT hypothesis of depressive disorder is supported by vast amounts of data that serotonin metabolism is altered in depression[55]. The shunt of Try from 5-HT

formation to Kyn formation is a dominating etiological factor of depression. Kyn was reported to be a proinflammatory metabolite in the neuroimmune signaling network mediating depressive-like behavior[56]. The Kyn/Try ratio, an indicator of the activation of the first step of the Kyn pathway, the elevation of which indicated a decrease in the conversion of tryptophan to 5-HT. Activation of the Kyn pathway via inflammation has been substantiated both in clinical and preclinical research[57, 58]. Inflammation-driven alterations in kynurenine metabolic pathways results in substantial alterations in the metabolism of 5-HT. Our study showed a low content of 5-HT on day 7 after AMI, accompanied with a rise in Kyn/Try ratio. Myocardial infarction might disturb tryptophan metabolism through the kynurenine pathway, thereby resulting in a decrease in 5-HT synthesis. PCF might change the expression of 5-HT directly via the kynurenine pathway, thus improving depression-like behaviors in AMI rats.

One of the most attractive features of hippocampus is the unusual capacity for adult neurogenesis. In the sub-granular zone of the dentate gyrus (DG) of the hippocampus, new-born neurons are continuously generated, developed into mature neurons and functionally integrated into the existing neural circuitry. It's now well established that adult hippocampal neurogenesis is decreased in rodent models of depression[59]. Pro-inflammatory cytokines are involved in immune system-to-brain communication by activating resident microglia in the brain. Activated microglia reduce neurogenesis by suppressing neuronal stem cell proliferation, promoting apoptosis of neuronal progenitor cells, and decreasing survival of newly developing neurons and their integration into existing neuronal circuits[60]. The process of neurogenesis is strongly stimulated by brain-derived neurotrophic factor (BDNF), a neurotrophic factor that modulates functional and structural plasticity in the central nervous system, thus affecting dendritic spines and adult neurogenesis. A mass of studies reported the association of a decrease in BDNF mRNA and protein levels in the hippocampus with an increase of susceptibility to develop depressive disorders[61, 62]. For synaptic plasticity, we observed the morphology and number of neurons in the hippocampus through Nissl staining. The experimental results showed that the neuronal body of the hippocampus in the AMI group is lost. In our study, the effects of the AMI model on the expression of synaptic-plasticity protein in the hippocampus were explored by western blotting. The decrease in BDNF might account in part for the depression-like behavior in AMI rats at 21 days postoperatively. The results were opposite for rats treated with PCF, although no significant statistical difference was found.

According to the theory of traditional Chinese medicine, blood stasis not only brings about obstructed meridian vessel, but also produces the stagnation of vital energy, thus characterized by chest pain and mental fatigue, respectively named as “Zhenxintong” (AMI) and “Yubing” (depression). PCF consists of four kinds of herbs, among which Salvia miltiorrhiza and Rhizoma chuanxiong could promote blood circulation to remove blood stasis, while Semen ziziphi spinosae and Lily bulbs could make the subjects vigorous and uplifting. There are some laboratory achievements for the molecule compounds of components in PCF consistent with the inflammatory mechanism obtained in our study. Our previous research suggested that PCF reduced the inflammatory reaction derived from myocardial ischemia, and changed the expression of neurotransmitters directly by modifying the expression of GAD67 to relieve depression[17]. The published literature showed that the tanshinone IIA and salvianolate, as bioactive chemical constitutes from the root of Salvia miltiorrhiza, have significant advantage in cardiovascular

protective effects, as well as the efficacy of anti-inflammatory and myocardial protective[63]. Ferulic acid, an important active ingredient in Ligusticum chuanxiong, proved to be antidepressive via increasing monoamine neurotransmitter levels in the hippocampus[64].

There are limitations to our study. S100A9 is a small calcium-binding protein of the S100 family that is expressed, in most biological settings, as a heterodimer complexed with its partner, S100A8. Future researches concentrating on the functional and pathological difference between the monomer and heterodimer are urgently needed. Moreover, nothing but *in vitro* evidence was provided that S100A9 triggered microglial activation through TLR4 pathway, yet animal experiments in which a biological metabolism is more similar to the human body remains absent.

Conclusion

Taken together, PCF, a modified TCM formula, promoted the recovery of cardiac function and improved depression-like behavior post-MI. The possible mechanism involved in the protective effects of PCF *in vivo* included the reduction of inflammation and apoptosis in the myocardium, as well as the inhibition of the Kyn pathway and a boost of neurogenesis in the hippocampal tissue. Our results identify S100A9 as a promoter of macrophage/microglia inflammation, with a central role in depressive disorder induced by AMI. The concept of a common modifier driving both myocardial and hippocampal immune response to AMI is novel, and of major significance for realizing the immunopathology of this disease. Indeed, the effects of short-term S100A9 blockade closely recapitulate the consequences of reduced inflammation on cardiac function and depression. PCF was also proved to be efficacious for targeting local and systemic inflammatory phase post-MI. *In vitro* experiments found that protein S100A9 promoted the production of proinflammatory cytokines in microglia via TLR4, while PCF serum inhibiting the release of S100A9 may provide a therapeutic approach in microglial-mediated neuroinflammatory diseases. These findings provide scientific evidence for the cardioprotective and antidepressant effects of PCF, as well as the inhibition of S100A9, particularly in the process of suppressing inflammation.

Footnotes

Supplementary data can be found online at http://proteomecentral.proteomexchange.org/cgi/GetDataset?ID=PXD027832. The mass spectrometry proteomics data have been deposited to the ProteomeXchange Consortium (http://proteomecentral.proteomexchange.org) via the iProX partner repository with the dataset identifier PXD027832.

Abbreviations

AI: apoptosis index; AMI: acute myocardial infarction; Arg-1: arginase-1; BDI: beck depression inventory; BDNF: brain-derived neurotrophic factor; BSA: bovine serum albumin; BZ: peri-infarct border zone; C34: TLR4 inhibitor; CD68: cluster of differentiation 68; DAPI: 4,6-diamino-2-phenyl indole; DCX:

doublecortin; DEPs: differentially expressed proteins; DG: dentate gyrus; DMEM: dulbecco's-modified eagle's medium; DMSO: dimethyl sulphoxide; ECG: electrocardiograph; ECL: enhanced chemiluminescence; FA: ferulic acid; FBS: fetal bovine serum; GABA: γ-aminobutyric acid; GAD67: glutamic acid decarboxylase-67; GAPDH: glyceraldehyde-3-phosphate dehydrogenase; GC-MS: gas chromatography-mass spectrometry; HE: haematoxylin and eosin; HRP: horseradish peroxidase; IBA1: ionized calcium binding adapter molecule 1; IL-1β: interleukin-1β; iNOS: inducible Nitric Oxide Synthase; IOD: integrated optical density; LAD: left anterior descending; LC-MS/MS: label-free liquid chromatography-tandem mass spectrometry; LVEF: left ventricular ejection fractions; LVFS: left ventricular fractional shortening; LViDd: left ventricular end-diastolic inner diameter; LViDs: left ventricular end-systolic inner diameter; LVEDV: left ventricular end-diastolic volume; LVESV: left ventricular end-systolic volume; Kyn: kynurenine; NF-κB: nuclear factor kappa-B; NO: nitric oxide; OFT: open-field test; PCF: psycho-cardiology formula (Shuangxinfang); PEG400: 40% polyethylene glycol 400; PVDF: polyvinylidene difluoride; RAGE: receptor of advanced glycation endproducts; S100A9: Ca2+ binding proteins belonging to the S100 family; SD: Sprague-Dawley; SSRI: selective serotonin reuptake inhibitors; TCM: traditional Chinese medicine; TLR4: toll-like receptor 4; TNF-α: tumor necrosis factor-α; Try: tryptophan; TSPO: translocator protein; TUNEL: TdT-mediated dUTP Nick-End Labeling.

Declarations

Funding

This research was supported by Beijing Natural Science Foundation Program (No. 7202126).

Acknowledgements

We are thankful for the support of the DongFang Hospital of Beijing University of Chinese Medicine.

Ethics approval and consent to participate

The study was approved by the Institutional Animal Care and Use Committee of University of Chinese Medicine, Beijing, China (ethical number: BUCM-4-2020091108-3141).

Consent for publication

Not applicable.

Competing interests

The authors declare that they have no competing interests.

Author contributions

Haibin Zhao and Chao Wang conceived the project, designed and supervised this study. Yize Sun and Jinyu Shi and carried out animal experiments. Jiqiu Hou and Zhuoran Tang assisted with the

establishment of the AMI model. Yize Sun and Zheyi Wang performed *in vitro* experiments, as well as sample preparation and detection. Zheyi Wang performed the statistical analysis. Yize Sun completed the manuscript. All authors approved the final version of the manuscript.

Availability of data and materials

The datasets used and/or analyzed during the current study are available from the corresponding author on reasonable request.

References

1. Feng L, Li L, Liu W, Yang J, Wang Q, Shi L, Luo M. Prevalence of depression in myocardial infarction: A PRISMA-compliant meta-analysis. Med (Baltim). 2019;98:e14596.
2. Smolderen KG, Buchanan DM, Gosch K, Whooley M, Chan PS, Vaccarino V, Parashar S, Shah AJ, Ho PM, Spertus JA. Depression Treatment and 1-Year Mortality After Acute Myocardial Infarction: Insights From the TRIUMPH Registry (Translational Research Investigating Underlying Disparities in Acute Myocardial Infarction Patients' Health Status). Circulation. 2017;135:1681–9.
3. Trajanovska AS, Kostov J, Perevska Z. Depression in Survivors of Acute Myocardial Infarction. Mater Sociomed. 2019;31:110–4.
4. Worcester MU, Goble AJ, Elliott PC, Froelicher ES, Murphy BM, Beauchamp AJ, Jelinek MV, Hare DL. Mild Depression Predicts Long-Term Mortality After Acute Myocardial Infarction: A 25-Year Follow-Up. Heart Lung Circ. 2019;28:1812–8.
5. de Jonge P, van den Brink RH, Spijkerman TA, Ormel J. Only incident depressive episodes after myocardial infarction are associated with new cardiovascular events. J Am Coll Cardiol. 2006;48:2204–8.
6. Wilkowska A, Rynkiewicz A, Wdowczyk J, Landowski J, Cubała WJ. Heart rate variability and incidence of depression during the first six months following first myocardial infarction. Neuropsychiatr Dis Treat. 2019;15:1951–6.
7. AbuRuz ME, Al-Dweik G. Depressive Symptoms and Complications Early after Acute Myocardial Infarction: Gender Differences. Open Nurs J. 2018;12:205–14.
8. Rodrigues GH, Gebara OC, Gerbi CC, Pierri H, Wajngarten M. Depression as a Clinical Determinant of Dependence and Low Quality of Life in Elderly Patients with Cardiovascular Disease. Arq Bras Cardiol. 2015;104:443–9.
9. Gehi A, Haas D, Pipkin S, Whooley MA. Depression and medication adherence in outpatients with coronary heart disease: findings from the Heart and Soul Study. Arch Intern Med. 2005;165:2508–13.
10. Bangalore S, Shah R, Gao X, Pappadopulos E, Deshpande CG, Shelbaya A, Prieto R, Stephens J, Chambers R, Schepman P, McIntyre RS. Economic burden associated with inadequate antidepressant medication management among patients with depression and known cardiovascular diseases:

insights from a United States-based retrospective claims database analysis. J Med Econ. 2020;23:262–70.

11. Hawkins M, Schaffer A, Reis C, Sinyor M, Herrmann N, Lanctôt KL. Suicide in males and females with cardiovascular disease and comorbid depression. J Affect Disord. 2016;197:88–93.
12. Coupland C, Hill T, Morriss R, Moore M, Arthur A, Hippisley-Cox J. Antidepressant use and risk of cardiovascular outcomes in people aged 20 to 64: cohort study using primary care database. Bmj. 2016;352:i1350.
13. Kim JM, Stewart R, Lee YS, Lee HJ, Kim MC, Kim JW, Kang HJ, Bae KY, Kim SW, Shin IS, et al. Effect of Escitalopram vs Placebo Treatment for Depression on Long-term Cardiac Outcomes in Patients With Acute Coronary Syndrome: A Randomized Clinical Trial. Jama. 2018;320:350–8.
14. Iasella CJ, Kreider MS, Huang L, Coons JC, Stevenson JM. Effect of Selective Serotonin Reuptake Inhibitors on Cardiovascular Outcomes After Percutaneous Coronary Intervention: A Retrospective Cohort Study. Clin Drug Investig. 2019;39:543–51.
15. Kim Y, Lee YS, Kim MG, Song YK, Kim Y, Jang H, Kim JH, Han N, Ji E, Kim IW, Oh JM. The effect of selective serotonin reuptake inhibitors on major adverse cardiovascular events: a meta-analysis of randomized-controlled studies in depression. Int Clin Psychopharmacol. 2019;34:9–17.
16. Hou J, Shi J, An Y, Jin H, Jia J, Zhao H. The Clinical Research into Angina Pectoris Combined with Depression Treated with Shuangxin Prescription. Henan Traditional Chinese Medicine. 2019;39:224–7.
17. Wang C, Hou J, Du H, Yan S, Yang J, Wang Y, Zhang X, Zhu L, Zhao H. Anti-depressive effect of Shuangxinfang on rats with acute myocardial infarction: Promoting bone marrow mesenchymal stem cells mobilization and alleviating inflammatory response. Biomed Pharmacother. 2019;111:19–30.
18. Nagareddy PR, Sreejit G, Abo-Aly M, Jaggers RM, Chelvarajan L, Johnson J, Pernes G, Athmanathan B, Abdel-Latif A, Murphy AJ. NETosis Is Required for S100A8/A9-Induced Granulopoiesis After Myocardial Infarction. Arterioscler Thromb Vasc Biol. 2020;40:2805–7.
19. Wang Y, Zhang X, Duan M, Zhang C, Wang K, Feng L, Song L, Wu S, Chen X. Identification of Potential Biomarkers Associated with Acute Myocardial Infarction by Weighted Gene Coexpression Network Analysis. Oxid Med Cell Longev. 2021;2021:5553811.
20. Sakuma M, Tanaka A, Kotooka N, Hikichi Y, Toyoda S, Abe S, Taguchi I, Node K, Simon DI, Inoue T. Myeloid-related protein-8/14 in acute coronary syndrome. Int J Cardiol. 2017;249:25–31.
21. Marinković G, Grauen Larsen H, Yndigegn T, Szabo IA, Mares RG, de Camp L, Weiland M, Tomas L, Goncalves I, Nilsson J, et al. Inhibition of pro-inflammatory myeloid cell responses by short-term S100A9 blockade improves cardiac function after myocardial infarction. Eur Heart J. 2019;40:2713–23.
22. Ma L, Sun P, Zhang JC, Zhang Q, Yao SL. Proinflammatory effects of S100A8/A9 via TLR4 and RAGE signaling pathways in BV-2 microglial cells. Int J Mol Med. 2017;40:31–8.

23. Björk P, Björk A, Vogl T, Stenström M, Liberg D, Olsson A, Roth J, Ivars F, Leanderson T. Identification of human S100A9 as a novel target for treatment of autoimmune disease via binding to quinoline-3-carboxamides. PLoS Biol. 2009;7:e97.
24. Liang X, Xiu C, Liu M, Lin C, Chen H, Bao R, Yang S, Yu J. Platelet-neutrophil interaction aggravates vascular inflammation and promotes the progression of atherosclerosis by activating the TLR4/NF-κB pathway. J Cell Biochem. 2019;120:5612–9.
25. Kraakman MJ, Lee MK, Al-Sharea A, Dragoljevic D, Barrett TJ, Montenont E, Basu D, Heywood S, Kammoun HL, Flynn M, et al. Neutrophil-derived S100 calcium-binding proteins A8/A9 promote reticulated thrombocytosis and atherogenesis in diabetes. J Clin Invest. 2017;127:2133–47.
26. Stenström M, Nyhlén HC, Törngren M, Liberg D, Sparre B, Tuvesson H, Eriksson H, Leanderson T. Paquinimod reduces skin fibrosis in tight skin 1 mice, an experimental model of systemic sclerosis. J Dermatol Sci. 2016;83:52–9.
27. Tahvili S, Törngren M, Holmberg D, Leanderson T, Ivars F. Paquinimod prevents development of diabetes in the non-obese diabetic (NOD) mouse. PLoS One. 2018;13:e0196598.
28. Masouris I, Klein M, Dyckhoff S, Angele B, Pfister HW, Koedel U. Inhibition of DAMP signaling as an effective adjunctive treatment strategy in pneumococcal meningitis. J Neuroinflammation. 2017;14:214.
29. Adegoke EO, Adeniran SO, Zeng Y, Wang X, Wang H, Wang C, Zhang H, Zheng P, Zhang G. Pharmacological inhibition of TLR4/NF-κB with TLR4-IN-C34 attenuated microcystin-leucine arginine toxicity in bovine Sertoli cells. J Appl Toxicol. 2019;39:832–43.
30. Hou J, Wang C, Ma D, Chen Y, Jin H, An Y, Jia J, Huang L, Zhao H. The cardioprotective and anxiolytic effects of Chaihujialonggumuli granule on rats with anxiety after acute myocardial infarction is partly mediated by suppression of CXCR4/NF-κB/GSDMD pathway. Biomed Pharmacother. 2021;133:111015.
31. Oxenkrug G. Serotonin-kynurenine hypothesis of depression: historical overview and recent developments. Curr Drug Targets. 2013;14:514–21.
32. Muneer A. Kynurenine Pathway of Tryptophan Metabolism in Neuropsychiatric Disorders: Pathophysiologic and Therapeutic Considerations. Clin Psychopharmacol Neurosci. 2020;18:507–26.
33. Vancassel S, Capuron L, Castanon N. Brain Kynurenine and BH4 Pathways: Relevance to the Pathophysiology and Treatment of Inflammation-Driven Depressive Symptoms. Front Neurosci. 2018;12:499.
34. Maes M, Verkerk R, Bonaccorso S, Ombelet W, Bosmans E, Scharpé S. Depressive and anxiety symptoms in the early puerperium are related to increased degradation of tryptophan into kynurenine, a phenomenon which is related to immune activation. Life Sci. 2002;71:1837–48.
35. Zhang JC, Yao W, Hashimoto K. Brain-derived Neurotrophic Factor (BDNF)-TrkB Signaling in Inflammation-related Depression and Potential Therapeutic Targets. Curr Neuropharmacol. 2016;14:721–31.

36. Monteggia LM, Luikart B, Barrot M, Theobold D, Malkovska I, Nef S, Parada LF, Nestler EJ. Brain-derived neurotrophic factor conditional knockouts show gender differences in depression-related behaviors. Biol Psychiatry. 2007;61:187–97.
37. Li Y, Chen B, Yang X, Zhang C, Jiao Y, Li P, Liu Y, Li Z, Qiao B, Bond Lau W, et al. S100a8/a9 Signaling Causes Mitochondrial Dysfunction and Cardiomyocyte Death in Response to Ischemic/Reperfusion Injury. Circulation. 2019;140:751–64.
38. Sreejit G, Nagareddy PR. Response by Sreejit and Nagareddy to Letter Regarding Article, "Neutrophil-Derived S100A8/A9 Amplify Granulopoiesis After Myocardial Infarction". Circulation. 2020;142:e125–6.
39. Marinković G, Koenis DS, de Camp L, Jablonowski R, Graber N, de Waard V, de Vries CJ, Goncalves I, Nilsson J, Jovinge S, Schiopu A. S100A9 Links Inflammation and Repair in Myocardial Infarction. Circ Res. 2020;127:664–76.
40. Schiopu A, Cotoi OS. S100A8 and S100A9: DAMPs at the crossroads between innate immunity, traditional risk factors, and cardiovascular disease. Mediators Inflamm. 2013;2013:828354.
41. Ehrchen JM, Sunderkötter C, Foell D, Vogl T, Roth J. The endogenous Toll-like receptor 4 agonist S100A8/S100A9 (calprotectin) as innate amplifier of infection, autoimmunity, and cancer. J Leukoc Biol. 2009;86:557–66.
42. Riva M, Källberg E, Björk P, Hancz D, Vogl T, Roth J, Ivars F, Leanderson T. Induction of nuclear factor-κB responses by the S100A9 protein is Toll-like receptor-4-dependent. Immunology. 2012;137:172–82.
43. Ganta VC, Choi M, Farber CR, Annex BH. Antiangiogenic VEGF(165)b Regulates Macrophage Polarization via S100A8/S100A9 in Peripheral Artery Disease. Circulation. 2019;139:226–42.
44. Stankiewicz AM, Goscik J, Majewska A, Swiergiel AH, Juszczak GR. The Effect of Acute and Chronic Social Stress on the Hippocampal Transcriptome in Mice. PLoS One. 2015;10:e0142195.
45. Gong H, Su WJ, Cao ZY, Lian YJ, Peng W, Liu YZ, Zhang Y, Liu LL, Wu R, Wang B, et al. Hippocampal Mrp8/14 signaling plays a critical role in the manifestation of depressive-like behaviors in mice. J Neuroinflammation. 2018;15:252.
46. Yirmiya R, Rimmerman N, Reshef R. Depression as a microglial disease. Trends Neurosci. 2015;38:637–58.
47. Bengtsson AA, Sturfelt G, Lood C, Rönnblom L, van Vollenhoven RF, Axelsson B, Sparre B, Tuvesson H, Ohman MW, Leanderson T. Pharmacokinetics, tolerability, and preliminary efficacy of paquinimod (ABR-215757), a new quinoline-3-carboxamide derivative: studies in lupus-prone mice and a multicenter, randomized, double-blind, placebo-controlled, repeat-dose, dose-ranging study in patients with systemic lupus erythematosus. Arthritis Rheum. 2012;64:1579–88.
48. Boros F, Vécsei L. Progress in the development of kynurenine and quinoline-3-carboxamide-derived drugs. Expert Opin Investig Drugs. 2020;29:1223–47.
49. Huang S, Frangogiannis NG. Anti-inflammatory therapies in myocardial infarction: failures, hopes and challenges. Br J Pharmacol. 2018;175:1377–400.

50. Frangogiannis NG. Pathophysiology of Myocardial Infarction. Compr Physiol. 2015;5:1841–75.
51. Bah TM, Kaloustian S, Rousseau G, Godbout R. Pretreatment with pentoxifylline has antidepressant-like effects in a rat model of acute myocardial infarction. Behav Pharmacol. 2011;22:779–84.
52. Wann BP, Bah TM, Boucher M, Courtemanche J, Le Marec N, Rousseau G, Godbout R. Vulnerability for apoptosis in the limbic system after myocardial infarction in rats: a possible model for human postinfarct major depression. J Psychiatry Neurosci. 2007;32:11–6.
53. Bah TM, Benderdour M, Kaloustian S, Karam R, Rousseau G, Godbout R. Escitalopram reduces circulating pro-inflammatory cytokines and improves depressive behavior without affecting sleep in a rat model of post-cardiac infarct depression. Behav Brain Res. 2011;225:243–51.
54. Kraus C, Castrén E, Kasper S, Lanzenberger R. Serotonin and neuroplasticity - Links between molecular, functional and structural pathophysiology in depression. Neurosci Biobehav Rev. 2017;77:317–26.
55. Dell'Osso L, Carmassi C, Mucci F, Marazziti D. Depression, Serotonin and Tryptophan. Curr Pharm Des. 2016;22:949–54.
56. Zhang Q, Sun Y, He Z, Xu Y, Li X, Ding J, Lu M, Hu G. Kynurenine regulates NLRP2 inflammasome in astrocytes and its implications in depression. Brain Behav Immun. 2020;88:471–81.
57. Savitz J. The kynurenine pathway: a finger in every pie. Mol Psychiatry. 2020;25:131–47.
58. Troubat R, Barone P, Leman S, Desmidt T, Cressant A, Atanasova B, Brizard B, El Hage W, Surget A, Belzung C, Camus V. Neuroinflammation and depression: A review. Eur J Neurosci. 2021;53:151–71.
59. Tanti A, Westphal WP, Girault V, Brizard B, Devers S, Leguisquet AM, Surget A, Belzung C. Region-dependent and stage-specific effects of stress, environmental enrichment, and antidepressant treatment on hippocampal neurogenesis. Hippocampus. 2013;23:797–811.
60. Cope EC, Gould E. Adult Neurogenesis, Glia, and the Extracellular Matrix. Cell Stem Cell. 2019;24:690–705.
61. Weinstock M. Prenatal stressors in rodents: Effects on behavior. Neurobiol Stress. 2017;6:3–13.
62. Karege F, Perret G, Bondolfi G, Schwald M, Bertschy G, Aubry JM. Decreased serum brain-derived neurotrophic factor levels in major depressed patients. Psychiatry Res. 2002;109:143–8.
63. Li ZM, Xu SW, Liu PQ. Salvia miltiorrhizaBurge (Danshen): a golden herbal medicine in cardiovascular therapeutics. Acta Pharmacol Sin. 2018;39:802–24.
64. Zhang YJ, Huang X, Wang Y, Xie Y, Qiu XJ, Ren P, Gao LC, Zhou HH, Zhang HY, Qiao MQ. Ferulic acid-induced anti-depression and prokinetics similar to Chaihu-Shugan-San via polypharmacology. Brain Res Bull. 2011;86:222–8.

Figures

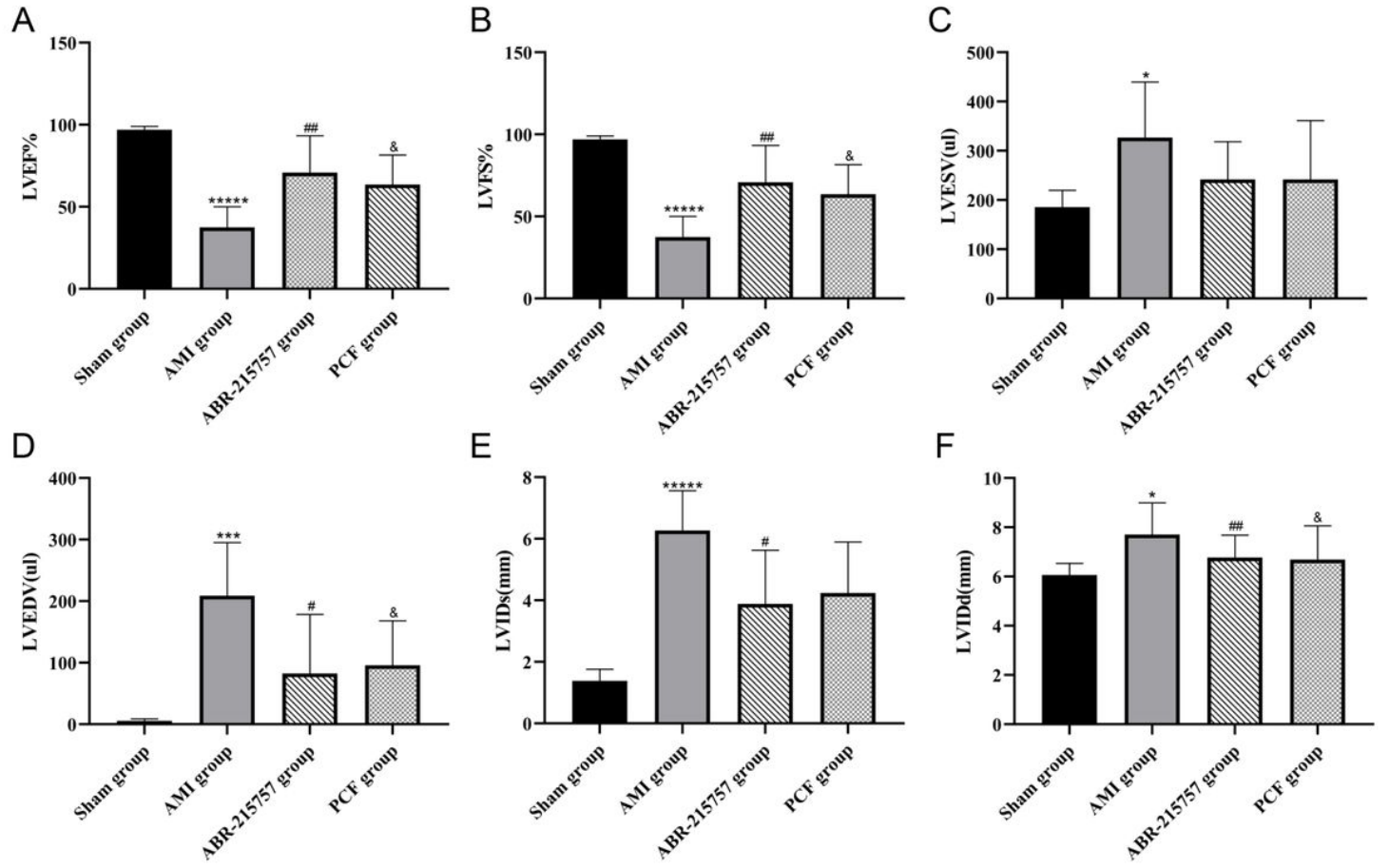

Figure 1

Cardiac function parameters of rats after myocardial infarction in echocardiography from each group (n=7). Values are expressed as mean ± SD. LVEF: left ventricular ejection fraction. LVFS: left ventricular fractional shortening. LViDd: left ventricular end-diastolic inner diameter; LViDs: left ventricular end-systolic inner diameter. LVEDV: left ventricular end-diastolic volume. LVESV: left ventricular end-systolic volume. * P < 0.05, *** P < 0.001, ***** P < 0.00001 compared with the sham group. # P< 0.05, ## P< 0.01, compared with the AMI group. & P < 0.05, compared with the AMI group.

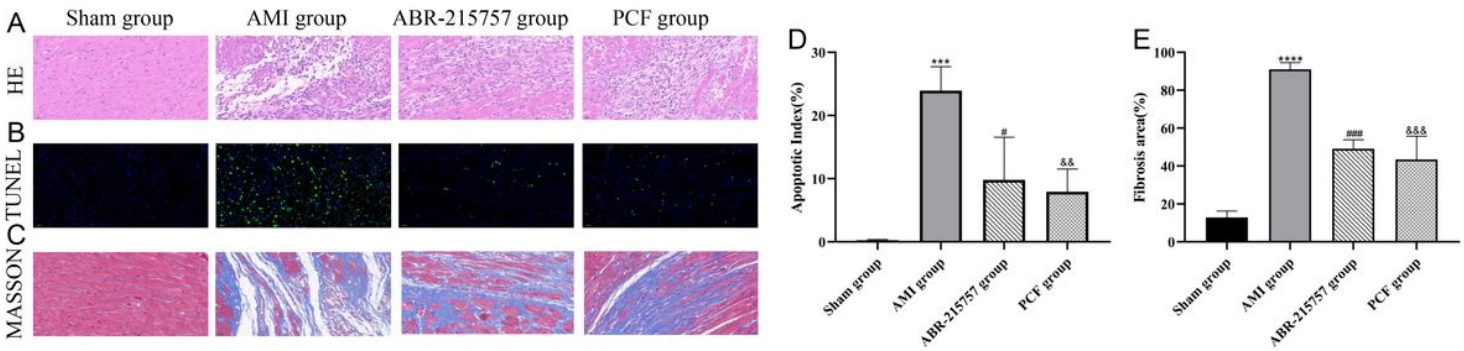

Figure 2

Effect of PCF on AMI-induced pathological changes in the myocardial tissue. (A) H&E staining showed different levels of inflammatory infiltration in the peri-infarct border zone. Scale bar, 40 μm. (B) TUNEL staining showed cardiac apoptosis on 7 days after MI surgery. Green staining of the nucleus indicated apoptosis, and blue staining marked DAPI. (C) Masson trichrome staining of heart slides at 21 days after MI. Red, myocardium; Blue, scarred fibrosis. (D) Quantitative analysis of TUNEL-positive cells in border zone of infarction area. Three separate fields were calculated from each group. (E) Fibrosis area as percentage (3 samples from each group). *** P < 0.001, ***** P < 0.00001 compared with the sham group. # P< 0.05, ### P< 0.001, compared with the AMI group. &&P < 0.01, &&&P < 0.001, compared with the AMI group.

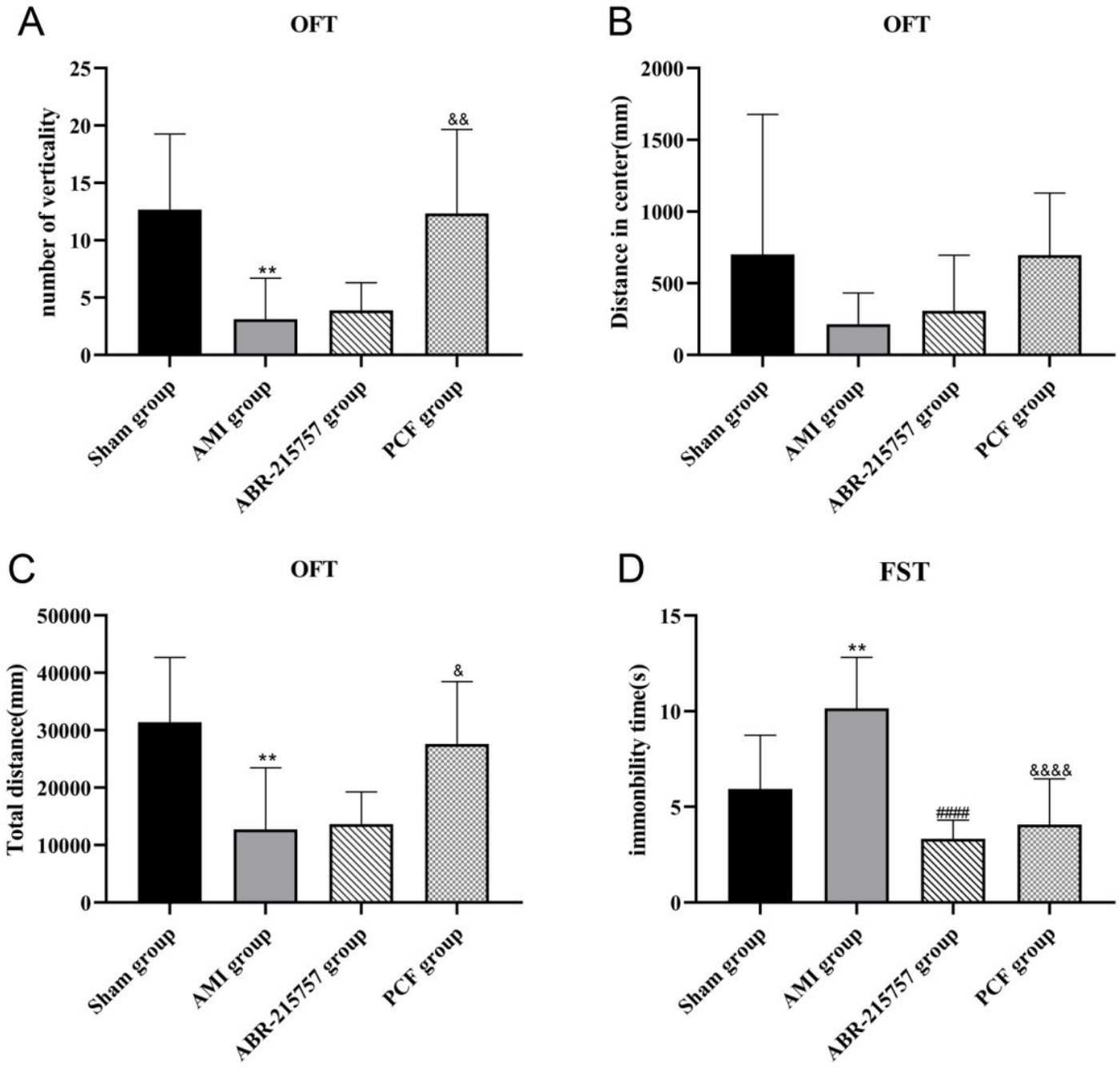

Figure 3

PCF significantly ameliorated depression-like behavior in rats after myocardial infarction. (A) Number of verticality in open field test (OFT). (B) distance in center, (C) total distance. (D) Immobility time of rats in forced swimming test (FST). n=9 per group. ** P < 0.01, compared with the sham group. #### P< 0.0001, compared with the AMI group. & P < 0.05, && P < 0.01, &&&& P < 0.0001, compared with the AMI group.

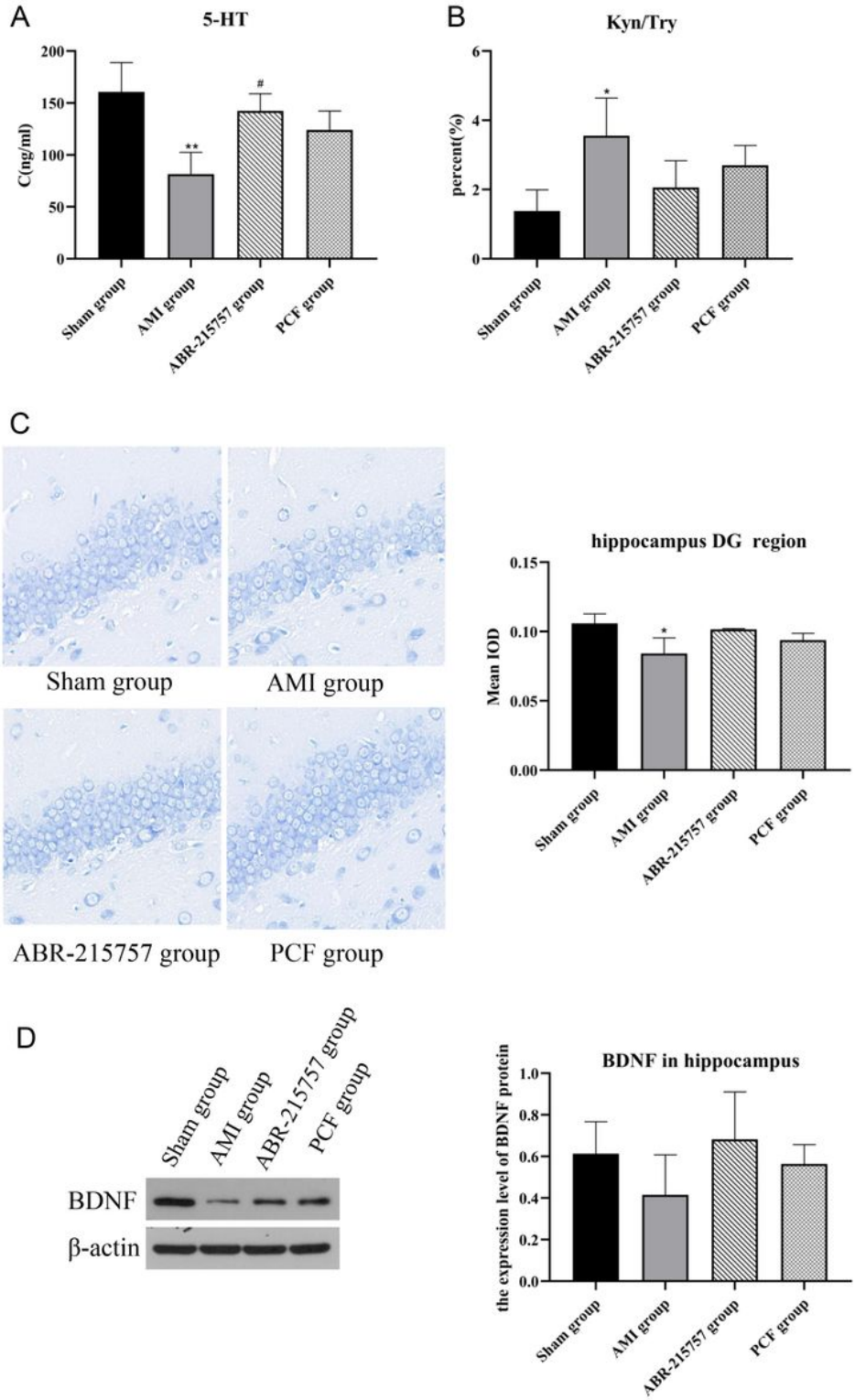

Figure 4

The effect of PCF on the neurotransmitter disorder and decreased neurogenesis caused by myocardial infarction. (A) HPLC analysis of 5-HT in the hippocampus of rats (n=3). (B) Ratio of kynurenine to tryptophan. (C) Nissl's staining in the dentate gyrus region of hippocampus from different groups. (D) Western blotting detected the protein expression levels of BDNF in the hippocampus (n=3). 5-HT: 5-hydroxytryptamine; Kyn: kynurenine; Try: tryptophan; BDNF: brain-derived neurotrophic factor; DG: dentate gyrus. *P < 0.05, ** P < 0.01, compared with the sham group. # P< 0.05, compared with the AMI group.

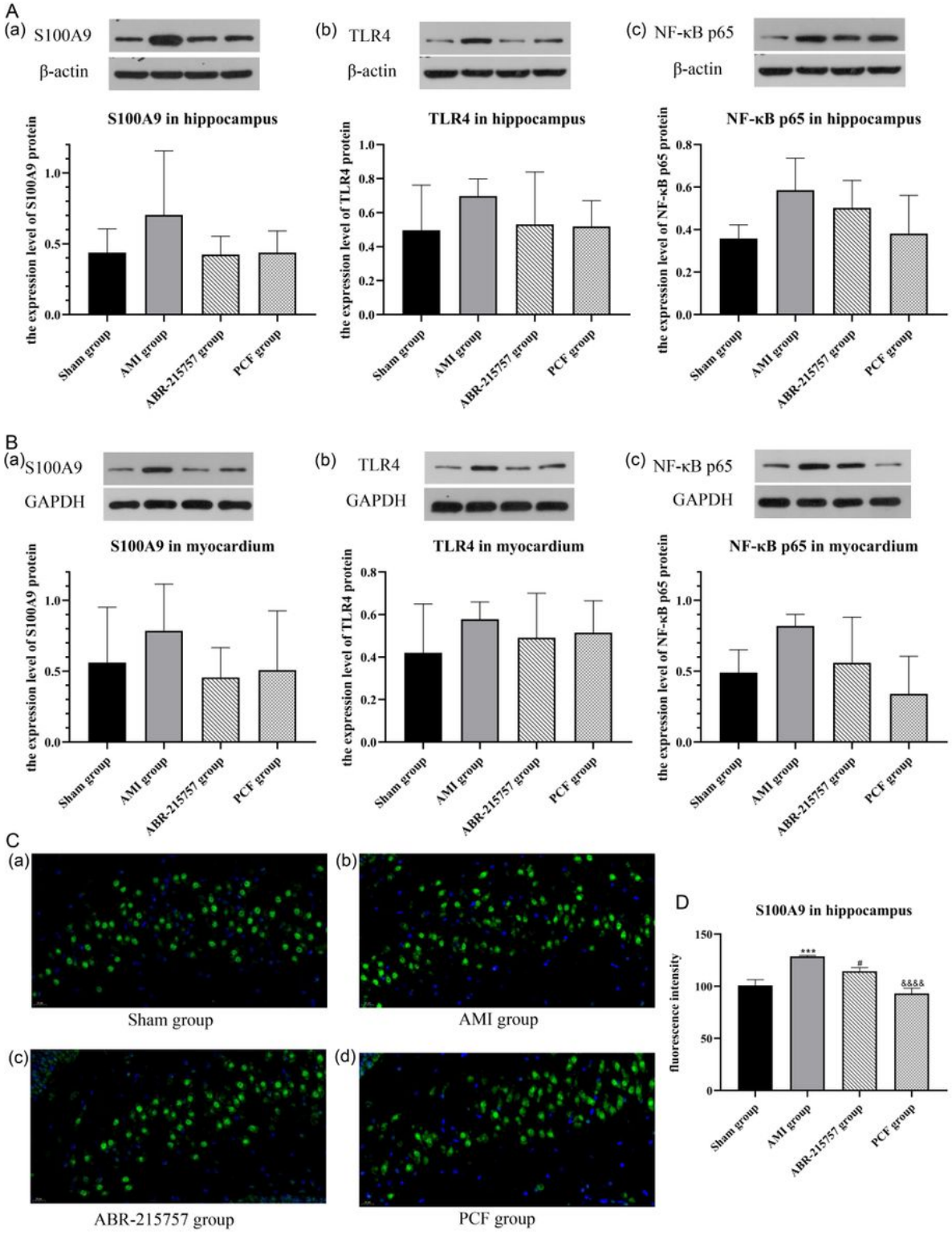

Figure 5

The effect of PCF on S100A9/TLR4/NF-κB pathway in the hippocampus and myocardium of AMI rats. (A) The protein bands of S100A9, TLR4 and NF-κB in the hippocampus detected by western blotting. Data are presented as mean ± SEM, n = 3 per group. (B) The protein bands of S100A9, TLR4 and NF-κB in the myocardium detected by western blotting. (C) Immunofluorescence analysis of S100A9 in hippocampus tissues. S100A9 immunostaining is shown in green, and DAPI in blue. (D) Mean optical density of S100A9-positive cells. Three fields were selected from each slide. *** P < 0.001 compared with the sham group. # P< 0.05 compared with the AMI group. &&&& P < 0.0001, compared with the AMI group.

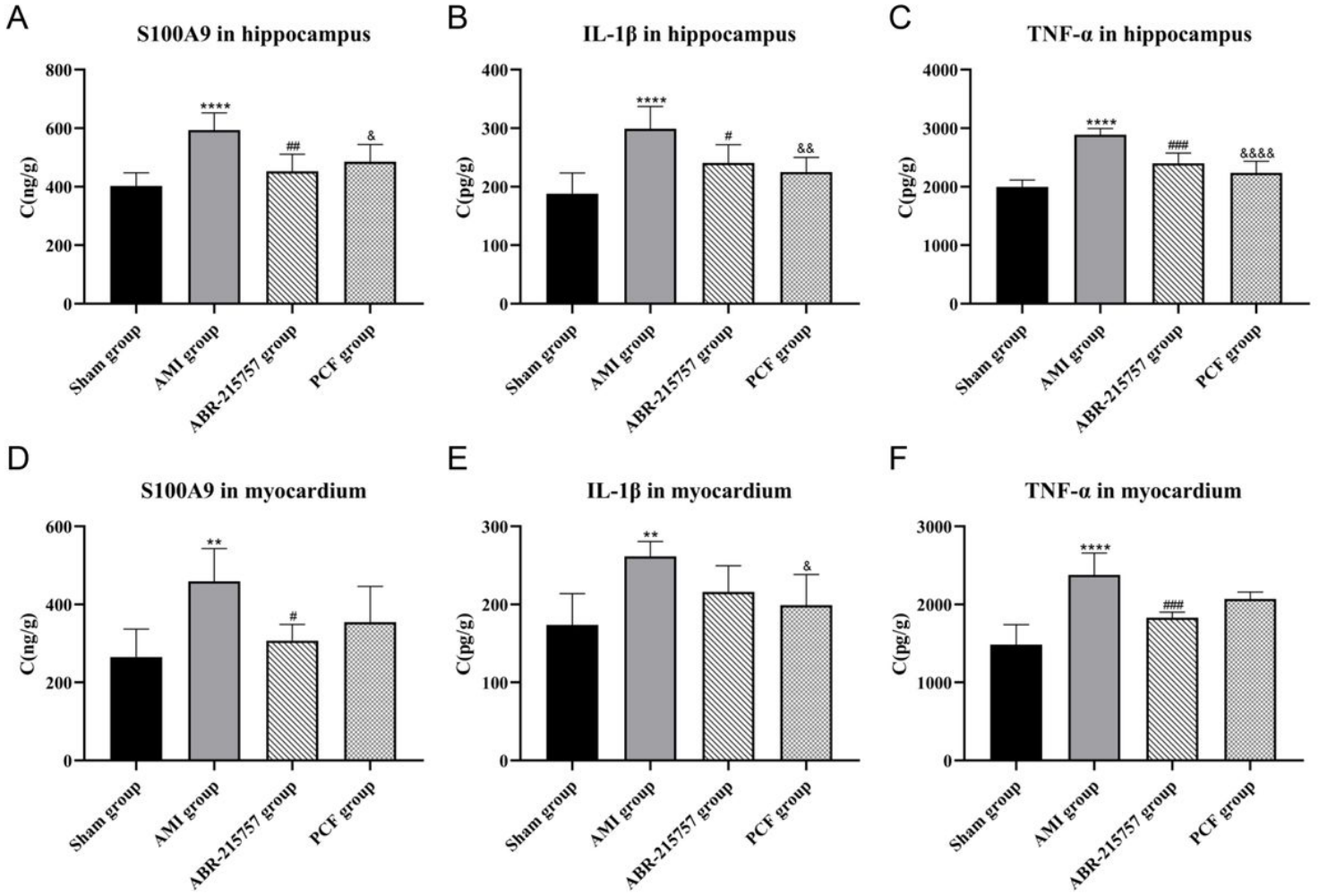

Figure 6

Levels of S100A9, IL-1β and TNF-α in the hippocampus and myocardium were determined by an ELISA assay. Values are expressed as mean ± SEM, n=6 per group. ** P < 0.01, **** P < 0.0001 compared with the sham group. # P< 0.05, ## P< 0.01, ### P< 0.001, compared with the AMI group. & P < 0.05, && P < 0.01, &&&& P < 0.0001, compared with the AMI group.

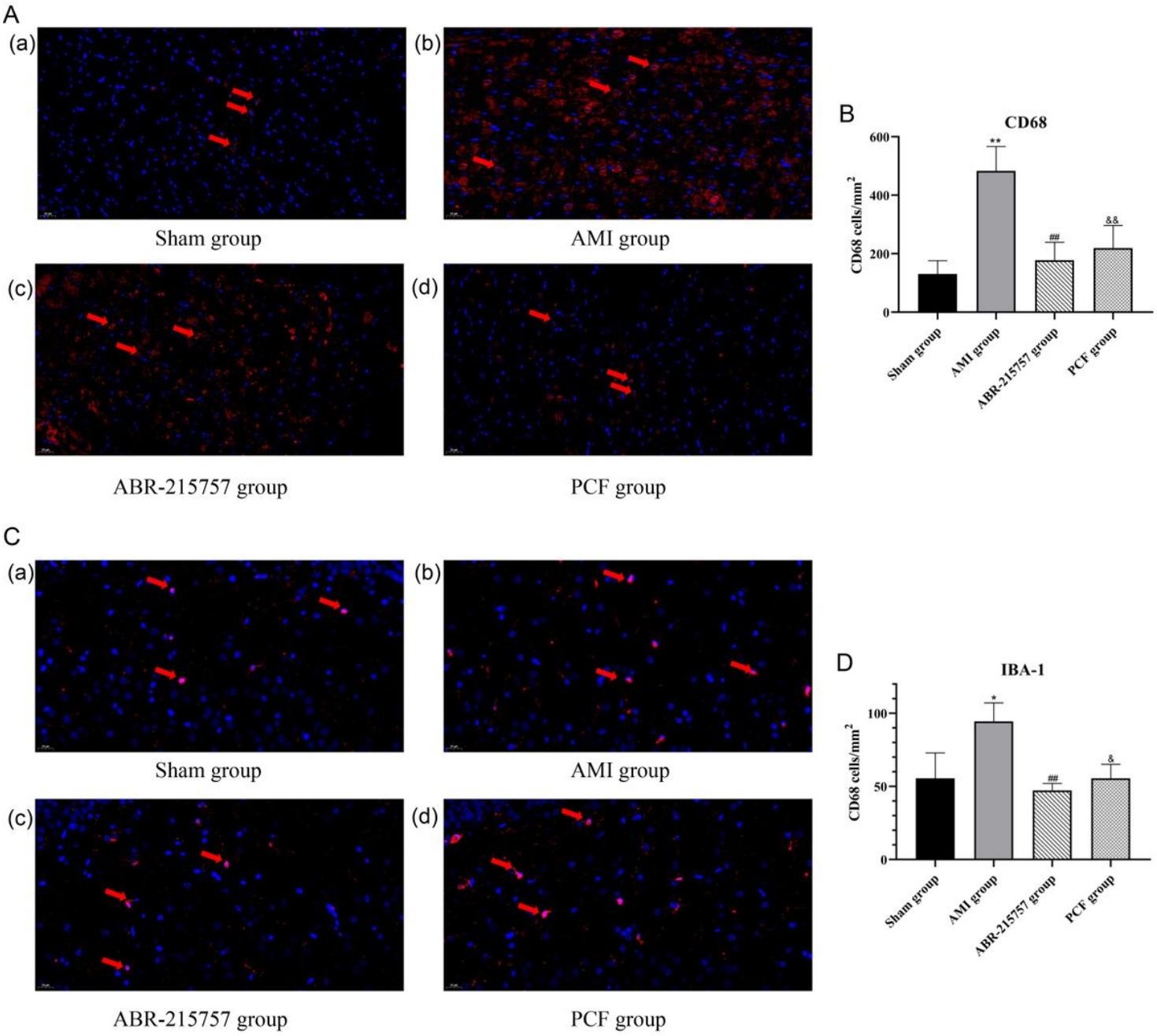

Figure 7

Macrophage activation in the myocardium and microglial activation in the DG region of AMI rats by immunofluorescence staining. (A) Representative images of CD68 positive cells in the myocardium. (B) Quantification of the CD68+ cell number. (C) Representative images of Iba-1 positive cells in the DG region of hippocampus. (D) Quantification of the Iba-1+ cell number. n=3 slices from each group. * $P < 0.05$, ** $P < 0.01$ compared with the sham group. ## $P < 0.01$, compared with the AMI group. & $P < 0.05$, && $P < 0.01$, compared with the AMI group.

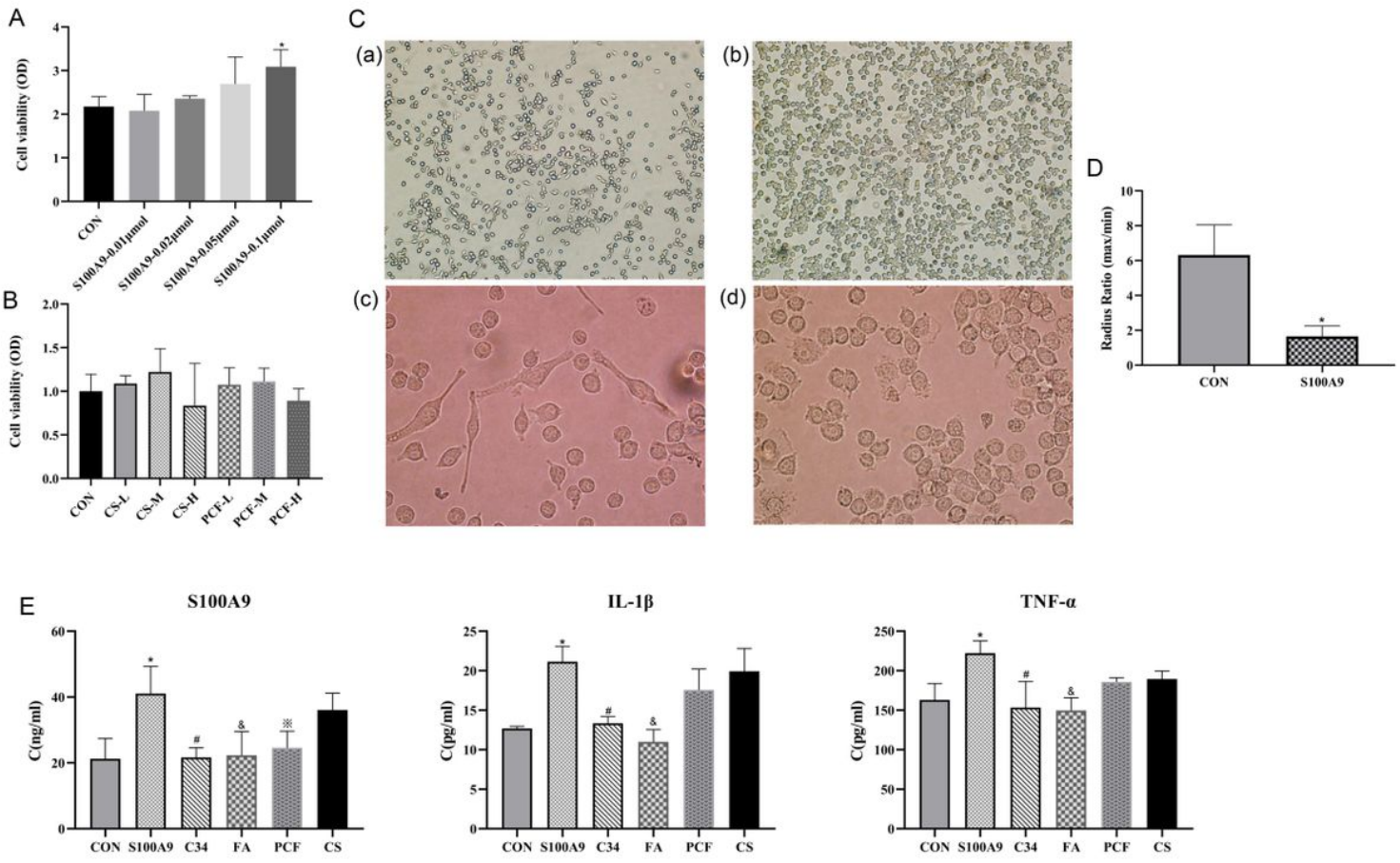

Figure 8

PCF serum reduced the proinflammatory effect of recombinant protein S100A9 in BV2 cells via inhibiting TLR4. (A) CCK-8 assay was used to detect the viability of BV2 cells. Microglia cells were treated with protein S100A9 (0.01,0.02, 0.05, 0.1μmol) for 6h. (B) Effect of PCF serum with concentration of 5%, 10% and 20% on the viability of BV-2 cells. (C) Morphological changes of BV2 microglia after incubation with S100A9 protein for 6h. (D) The ratio of the maximum radius to the minimum radius in BV2 microglia. (E) The level of S100A9, IL-1β and TNF-α in the culture media was measured with ELISA. Each value represents the mean ± SEM of three independent experiments. CS: control serum; CS-L: control serum low dose; CS-M: control serum medium dose; CS-H: control serum high dose; PCF: PCF serum; PCF-L: PCF serum low dose; PCF-M: PCF serum medium dose; PCF-H: PCF serum high dose; C34: TLR4 inhibitor; FA: ferulic acid; * $P < 0.05$, S100A9 group compared with the control group. # $P < 0.05$, C34 group compared with the S100A9 group. & $P < 0.05$, FA group compared with the S100A9 group. ※ $P < 0.05$, PCF group compared with the S100A9 group.